Energy Harvesting, Ride Comfort, and Road Handling of Regenerative Vehicle Suspensions

Lei Zuo[1]
e-mail: lei.zuo@stonybrook.edu

Pei-Sheng Zhang

Department of Mechanical Engineering,
State University of New York at Stony Brook,
Stony Brook, NY 11794-2300

This paper presents a comprehensive assessment of the power that is available for harvesting in the vehicle suspension system and the tradeoff among energy harvesting, ride comfort, and road handing with analysis, simulations, and experiments. The excitation from road irregularity is modeled as a stationary random process with road roughness suggested in the ISO standard. The concept of system H2 norm is used to obtain the mean value of power generation and the root mean square values of vehicle body acceleration (ride quality) and dynamic tire-ground contact force (road handling). For a quarter car model, an analytical solution of the mean power is obtained. The influence of road roughness, vehicle speed, suspension stiffness, shock absorber damping, tire stiffness, and the wheel and chasses masses to the vehicle performances and harvestable power are studied. Experiments are carried out to verify the theoretical analysis. The results suggest that road roughness, tire stiffness, and vehicle driving speed have great influence on the harvesting power potential, where the suspension stiffness, absorber damping, and vehicle masses are insensitive. At 60 mph on good and average roads, 100–400 W average power is available in the suspensions of a middle-sized vehicle. [DOI: 10.1115/1.4007562]

1 Introduction

When vehicles travel on the road, they are always subjected to excitation from road irregularities, braking forces, acceleration forces, and inertial forces on a curved track, which causes discomfort to the driver and influences maneuverability. Viscous shock absorbers, in parallel with suspension springs, have been widely used to reduce the vibration by dissipating the vibration energy into heat waste. To achieve better ride quality and road handling, active suspensions have been explored by many researchers [1]. However, it requires a significant amount energy, which limits its wide implementations. Hence, regenerative suspensions have been proposed, which has the potential to harvest energy from suspension vibration while reducing the vibration [2,3].

The initial theoretical research on the feasibility of vibration energy harvesting from vehicle suspension began two decades ago. Karnopp [4,5] examined the possibility of using a permanent magnetic motor as mechanical dampers for vehicles by dissipating the energy using variable resistors. Segel and Lu [6] analyzed the influence of highway pavement roughness on the vehicular resistance to motion due to tire and suspension damping, and they indicated that approximate 200 W of power are dissipated by dampers of a passenger car at 30 mph. Hsu [7] looked into the electrical active suspension with LQG control and estimated that up to 400 W of energy is recoverable at a highway driving condition, which is 5% of propulsion power to maintain GM impact at 60 mph. Abouelnour and Hammad [8] looked into the concept of energy and electro-mechanic suspension, and their simulation based on a quarter car model predicts that 150 W of energy dissipated by shock absorbers can be converted into electrical power at 56 mph. Goldner et al. [9] did some preliminary studies on the energy recovery in vehicles and claimed the recoverable energy for a 2500 lb vehicle with an average speed of 45 mph is about 20–70% (up to 7500 W) of the propulsion power on a typical highway. Kawamoto et al. [10] modeled a ball-screw type electromagnetic damper for active automobile suspension, and their experiments show a 15.3 W energy recovery from one shock absorber of a vehicle on Class C road at 50 mph, mainly from vibration above 2 Hz. Zhang et al. [11] tested a regenerative suspension with a ball screw and a three-phase motor of a real car on vibration test rig and obtained 11.7 W under random excitation or 46 W for four shock absorbers.

Although much initial work has been done in regenerative vehicle suspension regarding the power potential, the fundamental questions are still not clear: (1) What is the potential of harvestable power? The number in literature [4–11] varies in a very large range, from 46 W to 7500 W. (2) What is the relation of the power and the road roughness and driving speed? (3) How sensitive is the harvestable power to the changes of the vehicle parameters? (4) Will the ride quality (vibration intensity) and road handling (tire-ground contact force) be better if we extract more energy from the suspension system? These unanswered questions are very critical to understand the regenerative suspension and to guide the design of the regenerative shock absorbers. It is the purpose of this paper to address the above questions by creating a mathematical model for road-vehicle-suspension system and by systematically analyzing the vehicle dynamics, ride comfort, road handling, and potential power at the same time. An experimental study is also conducted.

2 Modeling of Vehicle and Road Dynamics

This section will discuss the modeling of the road-vehicle dynamics and the performance indices including energy, ride comfort, and road handing.

2.1 Quarter Car Model. As the vehicle travels on the road, the wheels follow the profile x_0 of the irregularity of the road surface, which become the main excitation sources of vehicle vertical vibration. Figure 1 (left) shows a quarter car model, which is modeled as a two-degree-of-freedom, with suspension stiffness k_2 and

[1]Corresponding author.

Contributed by the Design Engineering Division of ASME for publication in the JOURNAL OF VIBRATION AND ACOUSTICS. Manuscript received March 31, 2011; final manuscript received July 14, 2012; published online February 4, 2013. Assoc. Editor: Wei-Hsin Liao.

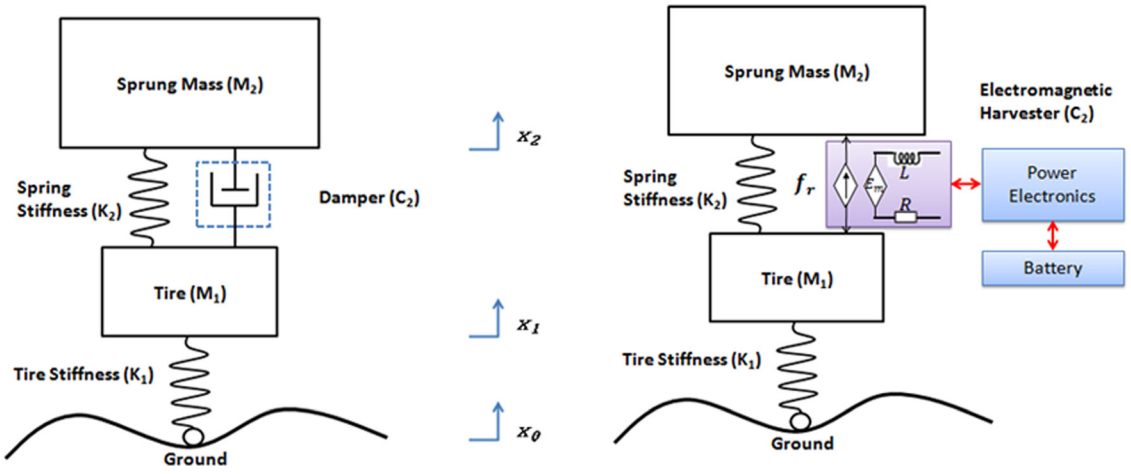

Fig. 1 Quarter-car model with viscous damper (left) and quarter-car model with electromagnetic harvester (right)

damping coefficient c_2, tire stiffness k_1, wheel mass m_1, and vehicle body mass m_2. The tire stiffness is usually small. The dynamic equation can be written as

$$\begin{bmatrix} m_1 & 0 \\ 0 & m_2 \end{bmatrix} \begin{pmatrix} \ddot{x}_1 \\ \ddot{x}_2 \end{pmatrix} + \begin{bmatrix} c_2 & -c_2 \\ -c_2 & c_2 \end{bmatrix} \begin{pmatrix} \dot{x}_1 \\ \dot{x}_2 \end{pmatrix} + \begin{bmatrix} k_1 + k_2 & -k_2 \\ -k_2 & k_2 \end{bmatrix} \begin{pmatrix} x_1 \\ x_2 \end{pmatrix} = \begin{bmatrix} k_1 \\ 0 \end{bmatrix} x_0 \tag{1}$$

Figure 1 (right) shows a quarter car model with a regenerative suspension where the viscous oil damper is replaced with an electromagnetic energy transducer. It can be shown that the electromagnetic shock absorber will appear to be an ideal viscous damper for an external resistive load (R_e) and negligible coil inductance (L) [12].

$$c_{\text{eq}} = \frac{M^2 k_e^2}{R + R_e} \tag{2}$$

where k_e and k_t are, respectively, the back EMF voltage and force constant of the transducer, and M is the motion amplification of the motion transmission. With the regenerative suspension system, the vibration energy can be converted into electricity and at the same time the desired damping c_2 can be provided. The electricity is stored in a battery after power regulation using power electronics, which can be further used for self-powered active or semi-active vibration control.

2.2 Road Roughness. The road irregularity is random, varying in a wide range. The road roughness is typically represented as a stationary Gaussian stochastic process of a given displacement power spectral density (PSD) in $\text{m}^2/(\text{cycle/m})$ [13–15]:

$$S_{\text{PSD}}(v) = S_0 v^{\beta} / v_0^{\beta} = G_r v^{\beta}, \quad \left[\frac{m^3}{\text{cycle}}\right] \tag{3}$$

where v is the spatial frequency in cycle/m, v_0 is the reference spatial frequency $v_0 = 1/2\pi$ (cycle/m), S_0 is the displacement PSD at v_0, $G_r = S_0/v_0^{\beta}$ is the road-roughness coefficient, and the exponent β is commonly approximated as – 2. Throughout numerous measurements, the international standard organization (ISO) suggests a road classification scheme based on the value of S_0, as shown in Table 1 [13–15].

The disturbance of road displacement input now can be modeled as white noise input through a first order filter. When a vehicle is driven at a speed V, the temporal excitation frequency ω and the spatial excitation frequency v are related by $\omega = 2\pi V v$ and $S_{\text{PSD}}(\omega)d\omega = S_{\text{PSD}}(v)dv$. And, the power spectral density of road excitation in terms of temporal frequency can be obtained as

Table 1 Degree of road roughness S_0 in $\text{m}^2/(\text{cycle/m})$ at reference spatial frequency $v_0 = 1/2\pi$ cycle/m suggested by ISO. Road-roughness coefficient $G_r = S_0/v_0^{-2}$.

Road class	S_0 range, $\times 10^{-6}$	S_0 mean, $\times 10^{-6}$
A (Very good)	<8	4
B (Good)	8–32	16
C (Average)	32–128	64
D (Poor)	128–512	256
E (Very Poor)	512–2048	1024
F	2048–8192	4096
G	8192–32768	16,384
H	>32768	

$$S_{\text{PSD}}(\omega) = \frac{2\pi G_r V}{\omega^2 + \omega_0^2} \tag{4}$$

A small cutoff frequency ω_0 is added to limit the displacement to be finite at vanishingly small spectral frequencies. Therefore, this displacement disturbance x_0 to the vehicle tire can be represented by a *unit-intensity white noise* signal $w(t)$ passing through a first-order filter given by

$$G(s) = \frac{\sqrt{2\pi G_r V}}{s + \omega_0} \tag{5}$$

Since ω_0 is very small, Eq. (5) also indicates that the ground velocity input $\dot{x}_0$ is a white noise with intensity of $2\pi G_r V$, which is proportional to the road roughness coefficient G_r and vehicle driving speed V.

$$E[\dot{x}_0(t)] = 0, \quad E[\dot{x}_0(t)\dot{x}_0(t+\tau)] = 2\pi G_r V \delta(\tau) \tag{6}$$

2.3 Ride Comfort. Ride comfort is subjective to human perception. Study has shown that human perception greatly depends on acceleration level, frequency, direction, and location. The ISO 2631 standard [16] specifies a method of evaluation of the effect of exposure to vibration on humans by weighting the root mean square (RMS) acceleration with human vibration-sensitivity curves. Such a low order filter has been designed by Zuo and Nayfeh [17] for vertical vibration.

$$H_{2631}(s) = \frac{80.03\,s^2 + 989\,s + 0.02108}{s^3 + 78.92\,s^2 + 2412\,s + 5614} \tag{7}$$

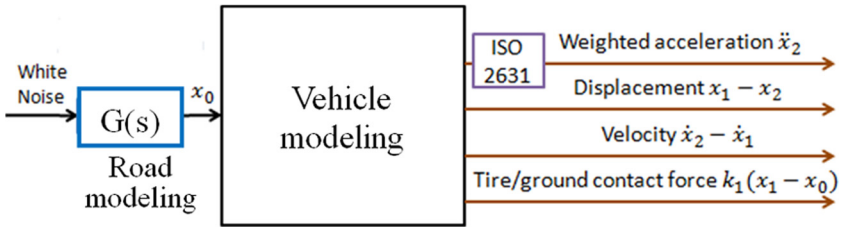

Fig. 2 Block diagram view of overall road-vehicle dynamics

In the quarter car model, the seat dynamics are not considered. Therefore, the ride comfort will be evaluated as the RMS value of the acceleration of the vehicle body (instead of human body) weighted by the ISO 2631 filter.

2.4 Road Handling and Safety. Under severe vibration, the wheel may not experience enough contact force with the ground or even lose contact, which will cause the vehicle to lose control during steering, propulsion, or braking. Hence, road handling is also considered an important performance index. It depends on the dynamic and static contact force between tire and ground. When the car is driving, the total contact force is consisting of static and dynamic loads. At higher dynamic force, the vehicle is unlikely to be handled safely. The wheel will lose ground contact when the ratio of dynamic and static contact forces is equal to or greater than 1. Therefore, the road handling index is defined as the ratio between dynamic loads to static load.

$$\eta_{RS} = k_1(x_1 - x_0)/(m_1 + m_2)g \tag{8}$$

Since the road roughness is random, the road handling is evaluated with a statistical quantity, which is the RMS value of the dynamic/static force between tire and ground.

2.5 Power Harvesting. The max energy that is available for harvesting is the amount that is dissipated by the viscous damping c_2 or extracted by c_{eq}. The instant damping force is proportional to the suspension velocity $(\dot{x}_2 - \dot{x}_1)$, and the instant power is the force times the suspension velocity $(\dot{x}_2 - \dot{x}_1)$. Therefore, the instant power dissipation is

$$P = c_2(\dot{x}_2 - \dot{x}_1)^2 \tag{9}$$

The average power in the shock absorber is hence proportional to the *mean square* (not RMS) of the suspension velocity. Power harvesting over this among will yield a suspension with a damping coefficient more than the desired value.

2.6 Performances as System H2 Norms. Figure 2 illustrates the block diagram including the road dynamics, vehicle dynamics, and performance indices. And the state space description of the overall system can be obtained. Note that the system input is unit white noise.

In linear system theory, the H_2 norm is the RMS value of the output under white noise input with unit intensity [18]. Therefore, we can use the concept of H_2 norm to obtain the weighted RMS acceleration of the vehicle body (ride comfort), the RMS value of the dynamic/static force between tire and ground (road handling), and the mean square valuate of the suspension velocity (thus, average power).

$$\sigma^2 = \|H\|_2^2 = \frac{1}{2\pi}\int_0^\infty \text{trace}(H^*(j\omega)H(j\omega))d\omega \tag{10}$$

where H is the transfer function from unit white noise input to the performance output. In state space realization, the H_2 norm can be efficiently computed by solving a linear Lyapunov equation.

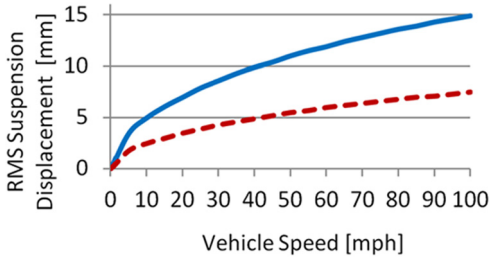

Fig. 3 Displacement analysis over vehicle speeds: on good road (dashed) and average road (solid)

When ω_0 in Eq. (5) is very small, the transfer function of suspension velocity and dynamics tire force is just a second order equation, and their RMS values can be evaluated analytically using the residue method, which will be detailed in Sec. 3.1.

3 Analysis and Simulation Results

In this section, the analysis based on a typical passenger car's parameters will be carried out. The nominal parameters of the quarter car are adapted from the literature [13]: wheel mass $m_1 = 40$ kg, vehicle body mass $m_2 = 362.7$ kg, tire stiffness $k_1 = 182{,}087$ N/m, suspension stiffness $k_2 = 20{,}053$ N/m, and suspension damping coefficient $c_2 = 1388$ N-s/m. Since most of the U.S. highways and freeways fall into average and good road categories, in these studies the road roughness coefficient G_r value is chosen as 64×10^{-7} and 16×10^{-7}, respectively, according to the ISO Class C and B roads.

3.1 Suspension Displacement, Velocity, and Power. Figures 3 and 4 show the RMS value of suspension displacement and velocity at a vehicle speed range of 0–100 mph. The RMS suspension velocity is 0.1–0.15 and 0.2–0.3 m/sec when a vehicle is traveling on good (Class B) and average (Class C) roads at 30–70 mph.

Figure 5 shows the harvestable power at different vehicle speeds. We see 100–400 W of power is dissipated, or potentially harvested, through the four shock absorbers when the middle-size passenger vehicle is traveling on a good and average road at

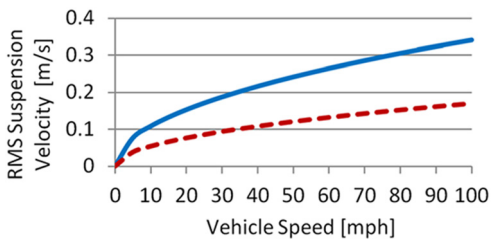

Fig. 4 Velocity analysis over vehicle speeds: on good road (dashed) and average road (solid)

60 mph. It should be noted that a car alternator of a typical car is about 500–600 W with an efficiency of 50–60% driven by the crankshaft. Also, as noted in Ref. [19], the average power 390 W recovery of electricity corresponds to a 4% fuel efficiency increase.

Since the ω_0 in Eq. (5) is negligibly small and the velocity excitation can be modeled as white noise of intensity $2\pi G_r V$ (Eq. (6)), the average power from a quarter car can be analytically obtained as follows. The transmission from ground velocity to the suspension velocity can be written as

$$\frac{\dot{x}_2 - \dot{x}_1}{\dot{x}_0} = \frac{k_1 m_2 \omega^2}{[(k_1 - m_1\omega^2)(k_2 - m_2\omega^2) - m_2 k_2 \omega^2] + j\omega c_2 (k_1 - m_1\omega^2 - m_2\omega^2)} \tag{11}$$

Therefore, the RMS can be obtained using the residue theorem or the integration formula [20],

$$\sigma_{\dot{x}_2 - \dot{x}_1} = \left[\frac{1}{2\pi}\int_0^\infty 2\pi G_r V \left|\frac{\dot{x}_2 - \dot{x}_1}{\dot{x}_0}\right|^2 d\omega\right]^{1/2} = \sqrt{\frac{\pi G_r V k_1}{c_2}} \tag{12}$$

From Eqs. (8) and (10), the mean power in the suspension can be obtained,

$$P_{\text{ave}} = c_2 \sigma^2_{\dot{x}_2 - \dot{x}_1} = \pi G_r V k_1 \tag{13}$$

Hence, an important observation is that the mean power in the suspension due to road roughness is proportional to the roughness coefficient G_r, the vehicle travel speed V, and the tire stiffness k_1. It has nothing to do with the suspension stiffness or damping, sprung or unsprung masses. This conclusion is based on the assumption that the road velocity due to road roughness is white noise, whose intensity is proportional to the roughness coefficient G_r and the vehicle travel speed V. Due to the flatness of the white noise spectrum, a high vehicle travel speed will increase the excitation at all frequencies uniformly, resulting an average power independent of the mechanical low-pass filter effect (Eq. (11)).

3.2 Ride Comfort and Road Handling. As mentioned, the ride comfort is measured by the RMS value of the vehicle body acceleration weighted by the human-vibration sensitivity curve. The result is shown in Fig. 6. It indicates the higher the vehicle speed, the larger vertical weighted acceleration will be, and hence, the less comfortable the ride will be. The same tendency happens to the road handling curve in Fig. 7; the ratio of the tire dynamic force over tire static force increase as the vehicle speed increases, which shows that at a higher speed or on rougher road, the vehicle has a higher risk of losing contact force between the tire and the ground and cause handling and safety hazards.

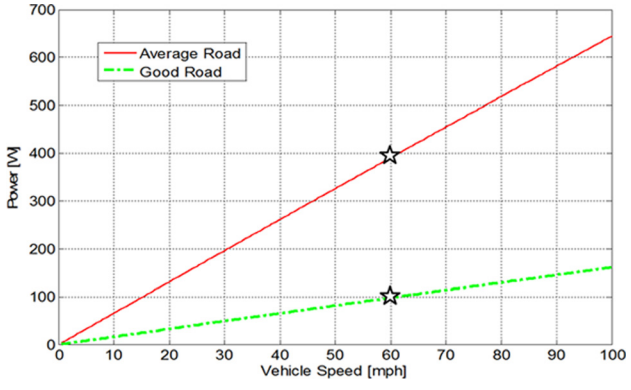

Fig. 5 Power potential in the suspension system of a typical passenger car at various vehicle speeds

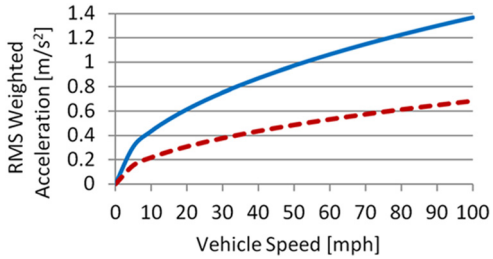

Fig. 6 Ride comfort at various vehicle speeds: on good road (dashed) and average road (solid)

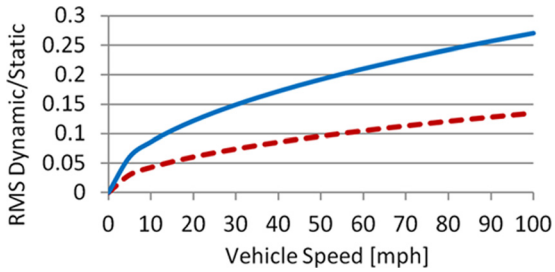

Fig. 7 Ride safety at various vehicle speeds on good road (dashed) and average road (solid)

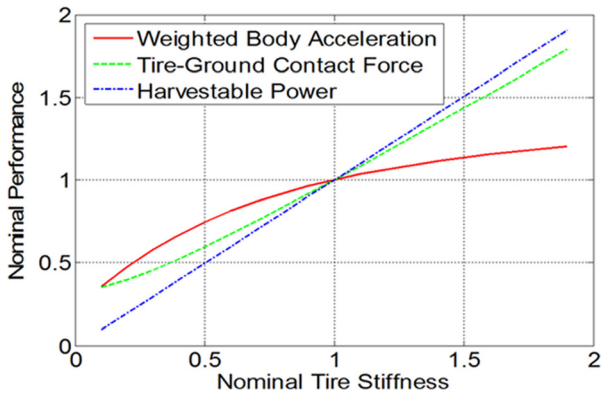

Fig. 8 Effects of tire stiffness on vehicle performances

Since the transmissions from ground velocity to vehicle body acceleration and tire deflection are only in the fourth order form

$$\frac{\ddot{x}_2}{\dot{x}_0} = \frac{k_1 k_2 j\omega - k_1 c_2 \omega^2}{[(k_1 - m_1\omega^2)(k_2 - m_2\omega^2) - m_2 k_2 \omega^2] + j\omega c_2 (k_1 - m_1\omega^2 - m_2\omega^2)} \tag{14}$$

$$\frac{x_1 - x_0}{\dot{x}_0} = \frac{-k_2(m_1+m_2)j\omega + c_2(m_1+m_2)\omega^2 + m_1m_2j\omega^3}{[(k_1 - m_1\omega^2)(k_2 - m_2\omega^2) - m_2k_2\omega^2] + j\omega c_2(k_1 - m_1\omega^2 - m_2\omega^2)} \tag{15}$$

an analytical solution to the RMS value of *unweighted* vehicle body acceleration and the RMS ratio of dynamic to static tire-ground contact forces can also be obtained, as in the Appendix.

3.3 Parameter Sensitivity Analysis. Further studies are conducted to investigate the sensitivities of ride comfort, road handing, and harvestable power to the vehicle parameter changes, including the masses of vehicle body and wheel, the suspension stiffness and damping, and tire stiffness. These studies are important to understand the tradeoff among power, ride comfort, and ride safety and to guide the design of regenerative suspensions.

Figures 8–10 plot the normalized performance to the changes of tire stiffness, wheel mass, and vehicle body mass, respectively. As we can see in Fig. 8, the change of tire stiffness has significant effects on the regenerated power. Neither the sprung nor unsprung mass has influence. The harvestable power increases linearly as tire stiffness increases (which can be the result of higher air pressure in the tire). However, a stiffer tire contributes negative effects to the ride comfort and road handling or safety. Figures 10 and 11 indicate that large vehicle body mass and small wheel mass are preferred for ride comfort and road handling.

To gain some physical insight, we plot the frequency responses from ground excitation velocity to suspension vibration velocity of the nominal and perturbed systems in Fig. 11. When the sprung mass increases, the first natural frequency decreases and the damping decreases too. The area increased at lower frequency is compensated by the decrease of the area above the first natural frequency; as a result the total area under the curve (RMS value of suspension velocity and mean power) does not change.

Figures 12 and 13 show the normalized performance to the changes of suspension damping and stiffness. The tradeoff between ride comfort and road handling is illustrated vividly. For instance, according to Fig. 12, the optimal damping for ride comfort is shown at 0.4 c_2 while it is 1.6 c_2 for best ride safety concern. The mean power is not sensitive to the suspension stiffness or the shock absorber damping. The reason is that when the shock absorber damping decreases the suspension velocity increases; as a result, the mean power $c_2\sigma^2_{\dot{x}_2-\dot{x}_1}$ does not change.

4 Experimental Assessment

Road tests of a vehicle were conducted to evaluate the energy potential and to verify the above analysis.

4.1 Experiment Setup. A systematic view of the experiment setup is shown in Fig. 14. Miles ZX40S all-electrical low-speed car (2007, Miles Automotive Group, Ltd.) is used as the test vehicle for on-road data collecting on the campus of Stony Brook University. It has a curb weight of 2398 lb (1088 kg), similar as a *super-compact car*. The max speed limit of this campus vehicle is

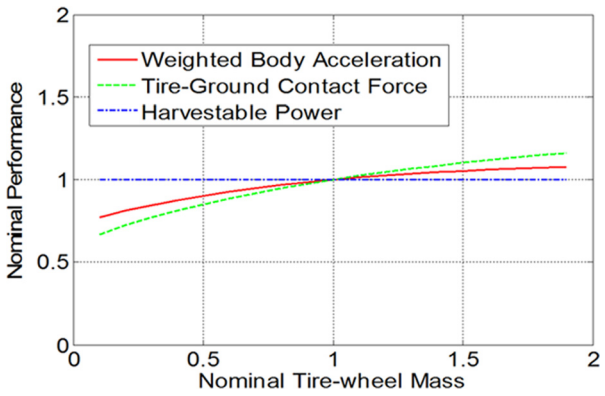

Fig. 9 Effects of tire-wheel mass on vehicle performances

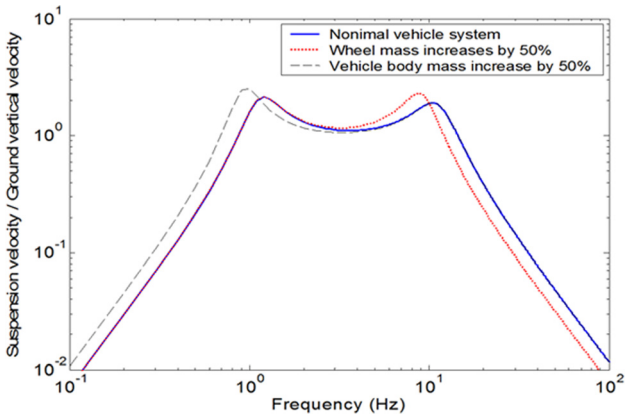

Fig. 11 Frequency response from ground to suspension velocities of nominal and perturbed vehicle system

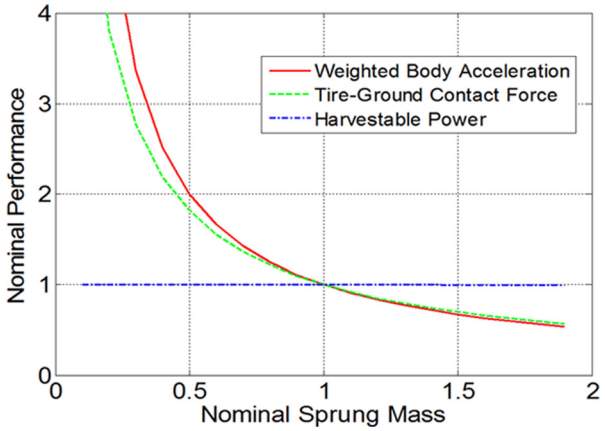

Fig. 10 Effects of sprung mass on vehicle performances

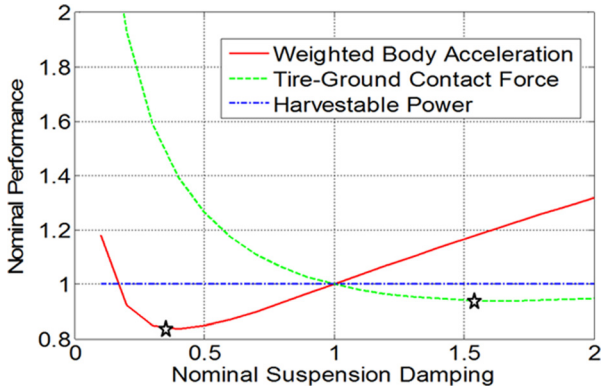

Fig. 12 Effects of suspension damping on vehicle performances

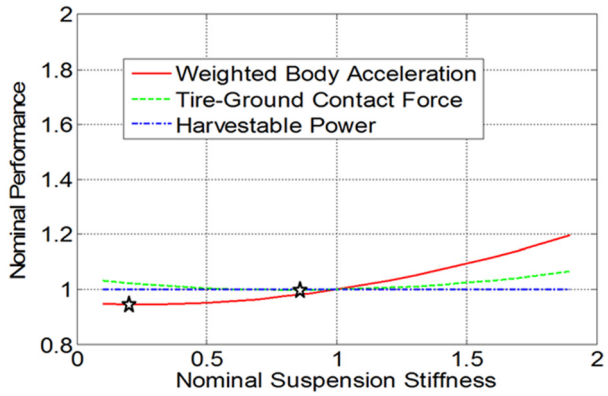

Fig. 13 Effects of suspension stiffness on vehicle performances

Fig. 14 Systematic view of experiment setup: road test of a super compact vehicle on Stony Brook campus road

25 mph. The tires are of 155/65R13. The shock absorber in the rear suspension is mounted at an angle about 30 deg to the vertical direction. Since there is no actual specification about the shock absorbers, we estimate that the rear shock absorber has a damping coefficient of 1995 N-s/m, corresponding to a typical suspension damping 1500 N-s/m in the vertical direction.

A Micro-Epsilon laser displacement sensor is mounted on the rear shock absorbers to measure its extension and compression, at a sampling frequency of 1000 Hz. The resolution of the sensor is 10 μm at 1 Hz and 50 μm at 1000 Hz. The profile of the shock absorber's compression during driving is recorded on a portable PC. The measurements are done at different vehicle speeds on the same section of campus road to make a fair comparison.

4.2 Suspension Displacement, Velocity, and Energy. Figure 15 shows a typical displacement profile obtained in the experiment at a vehicle speed of 25 mph. The instant peak to peak shock displacement can be as high as 40 mm, but the RMS value of this set of data is only 4.6 mm.

The suspension velocity is calculated from the measured displacement by taking the derivative and applying a fourth order Butterworth filter of bandwidth 0.1–100 Hz [21]. The velocity profile after filtering is plotted in Fig. 16. The peak instant velocity is 0.75 m/s, and the RMS value of the velocity profile is only 0.086 m/s.

Assume the damping coefficient is a constant, the instant power will be proportional to the shock absorber velocity square $P = c_2(\dot{x}_2 - \dot{x}_1)^2$. Since shock absorber velocity is a statistical process, the mean value of dissipated power is evaluated as

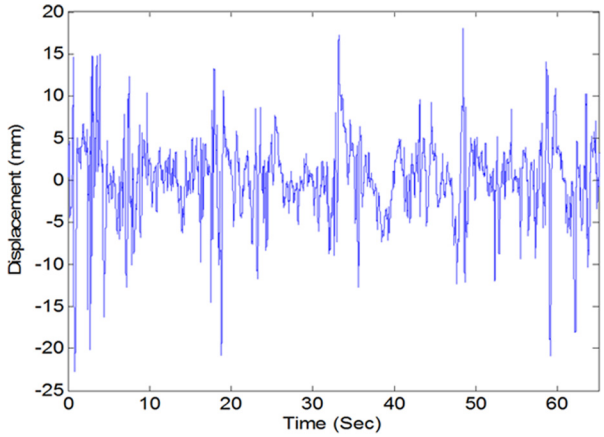

Fig. 15 Measured shock absorber displacements on a campus road at 25 mph. The RMS displacement is 4.6 mm.

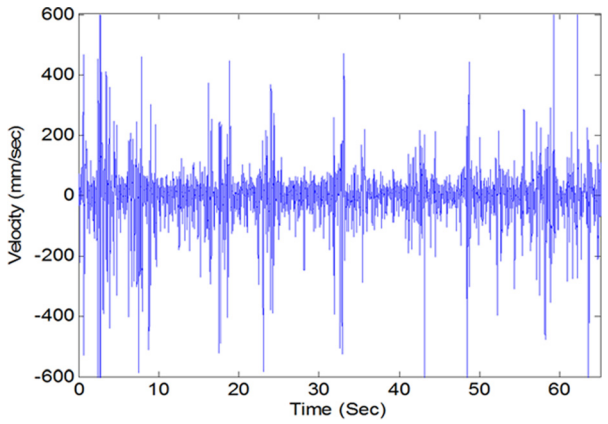

Fig. 16 Velocities of shock absorber compression and extension at vehicle speed of 25 mph on a campus road. The RMS velocity is 0.086 m/s.

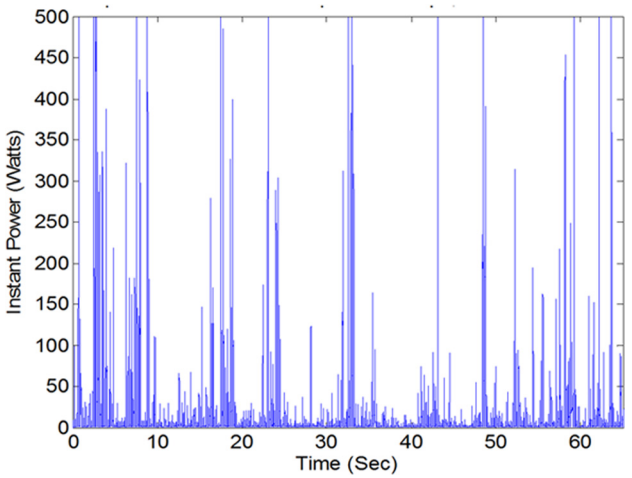

Fig. 17 Energy dissipation rate of one shock absorber at vehicle speed 25 mph on bitumen campus road, RMS = 14.6 W from one shock absorber

$$\bar{P} = \frac{1}{T}\int_0^T c_2(\dot{x}_2 - \dot{x}_1)^2 dt \tag{16}$$

Figure 17 shows the energy dissipation rate in one shock absorber on the campus road at 25 mph. The RMS power of one shock absorber is 14.6 W, and the total power of this *super-compact*

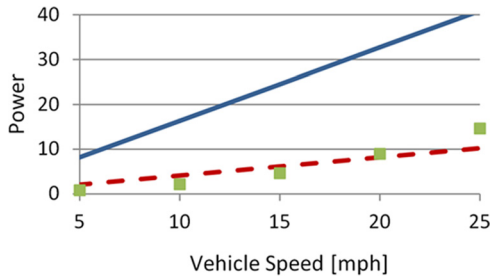

Fig. 18 Measured suspension power (squared) of one shock absorber in a super compact vehicle on campus road and theoretical predicted power of one shock absorber in a middle size car on good (dashed) and average road (solid)

vehicle will be 58 W at 25 mph on this campus road. Note that the instant peak power is on the order of kW at the peak velocity.

It also should be noted that the data in Figs. 15 and 16 are the displacement and velocity of the shock absorber itself. Since the shock absorber is not mounted vertically, the displacement and velocity of the suspension (in the vertical direction) should time $1/\cos(\theta)$, where θ is the angle between the shock absorber and the vertical spring axis. In the experiment setup, θ is about 30 deg. Therefore, the RMS suspension velocity at 25 mph should be $0.086/\cos(30\,\text{deg}) = 0.099$ m/sec. In the following discussion, we convert the shock absorber displacement and velocity to suspension vertical displacement and velocity so as to compare with the simulation results based on the quarter-car model.

4.3 Effect of Vehicle Speed on the Power. Further data was taken at 5 to 25 mph with a speed increment step of 5 mph. The suspension power at various travel speeds of the super compact vehicle is plotted in Fig. 18. We also plot the power of the theoretical predictions in Sec. 3, based on a typical middle sized car of total curb weight 3551 lb (1610.8 kg), which is 48% more than the test vehicle.

We wish to use the parameters of the super-compact car for the predictions, but unfortunately we do not have the parameter of suspension stiffness, tire stiffness, and wheel mass. If the natural frequencies and damping ratio of these two vehicles are the same, the tire stiffness of the middle size car should be 2.2 ($=1.48^2$) times as the test vehicle. So the energy data obtained in experiments in Fig. 18 should times 2.2 then compared with the predictions. The overall trends between experiment and prediction match well. The potential power increases slightly faster than the linear relation with speed. The reason is that the campus road is not straight and the vibration component due to centrifugal force increase linearly with the velocity square instead of velocity itself.

5 Conclusions

In this paper we assessed the power potential of the vehicle suspension induced by road irregularity and investigated the tradeoff among energy harvesting, ride comfort, and road handling. The ground irregularities are modeled as a stationary Gaussian stochastic process with certain roughness coefficients and power spectral density. The system H2 norm is used to evaluate the mean power in suspension, RMS weighted acceleration (ride comfort), and the RMS tire-ground contact force (road handling) at different vehicle speeds and road conditions. Quarter car model is employed but the H2 norm method can be applied to half or full car model. Analytical solution for mean value of power potential, RMS value of unweighted vehicle body acceleration, and RMS value of dynamics tire-ground contact force are obtained. Furthermore, sensitivity studies of vehicle performances on system parameters are illustrated graphically based on numeric calculation. We also tested a super-compact vehicle on the University campus road, by measuring the displacement of shock absorber and estimating the suspension power dissipation at various vehicle speeds. The experimental result matches the numerical results very well.

The following conclusions can be drawn from this study:

(1) A 100–400 W power potential (mean value) is available from the shock absorbers of a typical middle-sized passenger car at 60 mph on the good (Class B) and average (Class C) roads; on the road test of a super compact vehicle, 60 W energy potential is estimated at 25 mph speed on a campus road.
(2) The mean power potential depends on the road roughness G_r, vehicle speed V, and tires stiffness k_1. Under the common assumption that road displacement spectrum density is inverse proportional to the special frequency v square, or the road velocity spectrum is white noise, a simple linear relation exists, $P_{\text{ave}} = \pi G_r V k_1$, which is insensitive to the changes of suspension stiffness, shock absorber damping, vehicle sprung mass, or unsprung mass.
(3) Only tire stiffness has influence on power in the vehicle suspensions, while suspension stiffness and damping affect ride comfort and safety greatly; the tradeoff exists in suspension stiffness and damping between the optimal ride comfort and optimal road handling. Small unsprung mass and heavy sprung mass are preferred for ride comfort and road handling, but they have no effect on the power potential.
(4) At higher tire stiffness (such as larger tire pressure) the suspension dissipates more power, or the regenerative system harvests more power; however, the ride comfort and road handling will become worse. In this sense, more power harvesting does not mean better vibration reduction or better road handling. In additional, the influence of tire stiffness to the road rolling resistance should be considered too to fully evaluate the fuel efficiency of the vehicle.

Acknowledgment

The funding supports from New York State Energy Research and Development Authority (NYSERDA) and DOT's University Transportation Research Center (UTRC-II) are greatly appreciated. We wish to thank Jim O'Connor and David McAvoy of Stony Brook University Transportation Operations for offering the test vehicle and students Xiudong Tang, Annie Cheng, and Tao Ni for the assistance in road tests.

Appendix: Analytical Solution to RMS Values

When ω_0 in Eqs. (4) and (5) is small, the power spectrum the ground velocity excitation is of white noise of intensity $2\pi G_r V$ (Eq. (6)). Therefore, the RMS value of the vehicle body acceleration can be obtained using Eq. (14) as

$$\sigma_{\ddot{x}_2} = \left[\frac{1}{2\pi}\int_0^\infty 2\pi G_r V \left|\frac{\ddot{x}_2}{\dot{x}_0}\right|^2 d\omega\right]^{1/2} = \sqrt{\frac{\pi G_r V k_1}{m_2^2}\left[c_2 + \frac{k_1(m_1+m_2)}{c_2}\right]}$$

Similarly, the RMS ratio of dynamic to static tire-ground contact force can be obtained from Eq. (15),

$$\sigma_{\eta_{\text{RS}}} = \frac{k_1}{(m_1+m_2)g}\left[\frac{1}{2\pi}\int_0^\infty 2\pi G_r V \left|\frac{x_1 - x_0}{\dot{x}_0}\right|^2 d\omega\right]^{1/2} = \sqrt{\frac{\pi G_r V m_1 k_1}{(m_1+m_2)gc_2} + \frac{\pi G_r V}{k_1 m_2^2 g}\left[(m_1+m_2) + \frac{(m_1+m_2)^2 k_2^2}{c_2} - \frac{2m_1 m_2 k_2}{c_2^2}\right]}$$

References

[1] Sharp, R., and Crolla, D., 1987, "Road Vehicle Suspension System Design—A Review," Veh. Syst. Dyn., **16**(3), pp. 167–192.

[2] Zuo, L., Scully, B., Shestani, J., and Zhou, Y., 2010, "Design and Characterization of an Electromagnetic Energy Harvester for Vehicle Suspensions," Smart Mater. Struct., **19**(4), p. 045003.

[3] Zhang, Y., Yu, F., and Huang, K., 2009, "A State of Art Review on Regenerative Vehicle Active Suspension," Proceedings of the 3rd International Conference on Mechanical Engineering and Mechanics (ICMEM), Beijing, China, October 21–23.

[4] Karnopp, D., 1989, "Permanent Magnet Linear Motors Used as Variable Mechanical Dampers for Vehicle Suspensions," Veh. Syst. Dyn., **18**, pp. 187–200.

[5] Karnopp, D., 1992, "Power Requirement for Vehicle Suspension Systems," Veh. Syst. Dyn., **21**(1), pp. 65–71.

[6] Segel, L., and Lu, X.-P., 1982, "Vehicular Resistance to Motion as Influenced by Road Roughness and Highway Alignment," Aust. Road Res., **12**(4), pp. 211–222.

[7] Hsu, P., 1996, "Power Recovery Property of Electrical Active Suspension Systems," Proceedings of the 31st Intersociety Energy Conversion Engineering Conference, (IECEC 96), Washington, DC, August 11–16, pp. 1899–1904.

[8] Abouelnour, A., and Hammad, N., 2003, "Electric Utilization of Vehicle Damper Dissipated Energy," Al-Azhar Engineering Seventh International Conference (AEIC), Cairo, Egypt, April 7–10.

[9] Goldner, R., Zerigian P., and Hull, J., 2001, "A Preliminary Study of Energy Recovery in Vehicles by Using Regenerative Magnetic Shock Absorbers," SAE Paper No. 2001-01-2071.

[10] Kawamoto, Y., Suda, Y., Inoue, H., and Kondo, T., 2007, "Modeling of Electromagnetic Damper for Automobile Suspension," J. Syst. Des. Dyn., **1**, pp. 524–535.

[11] Zhang, Y., Huang, K., Yu, F., Gu, Y., and Li, D., 2007, "Experimental Verification of Energy-Regenerative Feasibility for an Automotive Electrical Suspension System," Proceedings of the IEEE International Conference on Vehicular Electronics and Safety, Beijing, China, December 13–15.

[12] Li, Z., Brindak, Z., and Zuo, L., 2011, "Modeling of an Electromagnetic Vibration Energy Harvester With Motion Magnification," Proceedings of the ASME International Mechanical Engineering Congress and Exposition (IMECE), Denver, CO, November 11–17, ASME Paper No. IMECE2011-65613, pp. 285–293.

[13] Zuo, L., and Nayfeh, S. A., 2003, "Structured H2 Optimization of Vehicle Suspensions Based on Multi-Wheel Models" Veh. Syst. Dyn., **40**(5), pp. 351–371.

[14] Taghirad, H., and Esmailzadeh, E., 1998, "Automobile Passenger Comfort Assured Through LQG/LQR Active Suspension," J. Vib. Control, **4**(5), pp. 603–618.

[15] Hong, K.-S., Sohn, H.-C., and Hedrick, J. K., 2002, "Modified Skyhook Control of Semi-Active Suspensions: A New Model, Gain Scheduling, and Hardware-In-The-Loop Tuning," ASME J. Dyn. Syst., Meas., Control, **124**, pp. 158–167.

[16] International Organization for Standardization, 1997, "ISO 2631-1:1997, Mechanical Vibration and Shock—Evaluation of Human Exposure to Whole-Body Vibration—Part 1: General Requirements," ISO, Geneva, Switzerland.

[17] Zuo, L., and Nayfeh, S. A., 2003, "Low Order Continuous-Time Filters for Approximation of the ISO 2631-1 Human Vibration Sensitivity Weightings," J. Sound Vib., **265**, pp. 459–465.

[18] Zhou, K., 1996, *Robust and Optional Control*, Prentice Hall, Upper Saddle River, NJ.

[19] Fairbanks, J., 2009, "Vehicular Thermoelectric Applications," Proceedings of the 15th Directions in Engine-Efficiency and Emissions Research (DEER) Conference, Dearborn, MI, August 3–6.

[20] Gradshtenyn, I. S., and Ryzhik, I. M., 1994, *Table of Integrals Series, and Products*, Academic Press, New York.

[21] Zhang, P. S., 2010, "Design of Electromagnetic Shock Absorbers for Energy Harvesting From Vehicle Suspensions," M.S. thesis, Stony Brook University, Stony Brook, NY.